Adsorption of Poly(ethylene oxide)-*b*-poly(ϵ-caprolactone) Copolymers at the Silica−Water Interface

P. Vangeyte,[†] B. Leyh,[‡] O. J. Rojas,[§] P. M. Claesson,[||,⊥] M. Heinrich,[#] L. Auvray,[¶,+] N. Willet,[†] and R. Jérôme*[,†]

Center for Education and Research on Macromolecules (CERM), University of Liège, Sart-Tilman B6a, B-4000 Liège, Belgium, Laboratoire de Dynamique Moléculaire, University of Liège, Sart-Tilman B6c, B-4000 Liège, Belgium, Department of Wood and Paper Science, North Carolina State University, Box 8005, Raleigh, North Carolina 27695, Department of Chemistry, Surface Chemistry, Royal Institute of Technology, Drottning Kristinas väg 51, SE-100 44 Stockholm, Sweden, Institute for Surface Chemistry, Box 5607, SE-114 86 Stockholm, Sweden, Forschungszentrum Jülich, Institut für Festkörperforschung, Postfach 1913, D-52425 Jülich, Germany, Laboratoire Léon Brillouin (CEA-CNRS), Saclay, 91 191 Gif sur Yvette, France, and Laboratoire Matériaux Polymères aux Interfaces (MPI), University of Evry, Bât. des Sciences, 91 025 Evry Cedex, France

Received October 19, 2004. In Final Form: January 27, 2005

The adsorption of amphiphilic poly(ethylene oxide)-*b*-poly(ϵ-caprolactone) and poly(ethylene oxide)-*b*-poly(γ-methyl-ϵ-caprolactone) copolymers in aqueous solution on silica and glass surfaces has been investigated by flow microcalorimetry, small-angle neutron scattering (SANS), surface forces, and complementary techniques. The studied copolymers consist of a poly(ethylene oxide) (PEO) block of M_n = 5000 and a hydrophobic polyester block of poly(ϵ-caprolactone) (PCL) or poly(γ-methyl-ϵ-caprolactone) (PMCL) of M_n in the 950−2200 range. Compared to homoPEO, the adsorption of the copolymers is significantly increased by the connection of PEO to an aliphatic polyester block. According to calorimetric experiments, the copolymers interact with the surface mainly through the hydrophilic block. At low surface coverage, the PEO block interacts with the surface such that both PEO and PCL chains are exposed to the aqueous solution. At high surface coverage, a dense copolymer layer is observed with the PEO blocks oriented toward the solution. The structure of the copolymer layer has been analyzed by neutron scattering using the contrast matching technique and by tapping mode atomic force microscopy. The experimental observations agree with the coadsorption of micelles and free copolymer chains at the interface.

Introduction

Polymer adsorption at solid/liquid interfaces is a topic of great interest, which in addition to scientific relevance finds application in very important technological and biological fields, including stabilization of colloidal dispersions (painting, detergency, and drug delivery) and surface modification (biocompatibility of artificial implants, wetting agents, etc.).[1,2] In this respect, diblock copolymers play a major role because one constitutive block may have high affinity for the surface, whereas the other block, with less or no affinity toward the surface, may protrude into solution. These copolymers can therefore act as stabilizers for solid dispersions[3] and, as a rule, provide the surface with new properties.

Theoretical[4−6] and experimental investigations[7−14] have contributed to the understanding of the adsorption of block copolymers. In aqueous solution, amphiphilic block copolymers are known to self-assemble into micelles in order to minimize the contact of water with the hydrophobic component. In the presence of a hydrophobic surface, adsorption of amphiphilic diblock copolymers can be driven by hydrophobic interactions.[2,8−11] When the surface is hydrophilic, the way the copolymer interacts is less obvious, as exemplified by the possible competition between water and hydrophilic silica for interaction with

* To whom correspondence should be addressed: fax (32)4-3663497; e-mail rjerome@ulg.ac.be.

[†] Center for Education and Research on Macromolecules (CERM), University of Liège.

[‡] Laboratoire de Dynamique Moléculaire, University of Liège.

[§] Department of Wood and Paper Science, North Carolina State University.

[||] Department of Chemistry, Surface Chemistry, Drottning Kristinas väg 51, Royal Institute of Technology.

[⊥] Institute for Surface Chemistry.

[#] Forschungszentrum Jülich, Institut für Festkörperforschung.

[¶] Laboratoire Léon Brillouin (CEA-CNRS).

[+] Laboratoire Matériaux Polymères aux Interfaces (MPI), University of Evry.

(1) Goddard, E. D. Applications of Polymer-Surfactant Systems. In *Interactions of Surfactants with polymers and Proteins*; Goddard, E. D., Ananthapadmanabhan, K. P., Eds.; CRC Press: Boca Raton, FL, 1993; Chapter 10.

(2) Jönsson, B.; Lindman, B.; Holmberg, K.; Kronberg, B. *Surfactants and Polymers in Aqueous Solution*; Wiley & Sons Ltd.: Chichester, 1998; Chapter 14.

(3) Bijsterbosch, H. D.; Cohen Stuart, M. A.; Fleer, G. J. *Macromolecules* **1998**, *31*, 9281.

(4) Schillen, K.; Claesson, P. M.; Malmsten, M.; Linse, P.; Booth, C. *J. Phys. Chem. B* **1997**, *101*, 4238.

(5) Marques, C. M.; Joanny, J. F.; Leibler, L. *Macromolecules* **1988**, *21*, 1051.

(6) Evers, O. A.; Scheutjens, J. M. H. M.; Fleer, G. J. *J. Chem. Soc., Faraday Trans.* **1990**, *86*, 1333.

(7) Yu, K.; Brinker, C. J.; Hurd, A. J.; Eisenberg, A. *Polym. Prepr.* **2001**, *42*, 659.

(8) Abraham, T.; Giasson, S.; Gohy, J. F.; Jérôme, R.; Muller, B.; Stamm, M. *Macromolecules* **2000**, *33*, 6051.

(9) Balastre, M.; Li, F.; Schorr, P.; Yang, J.; Mays, J. W.; Tirrell, M. V. *Macromolecules* **2002**, *35*, 9480.

(10) Lin, Y.; Alexandridis, P. *J. Phys. Chem. B* **2002**, *106*, 10834.

(11) Shar, J. A.; Obey, T. M.; Cosgrove, T. *Colloids Surf., A* **1998**, *136*, 21.

(12) Eskilsson, K.; Grant, L. M.; Hansson, P.; Tiberg, F. *Langmuir* **1999**, *15*, 5150.

(13) McDermott, D. C.; Lu, J. R.; Lee, E. M.; Thomas, R. K.; Rennie, A. R. *Langmuir* **1992**, *8*, 1204.

(14) Gellan, A.; Rochester, C. H. *J. Chem. Soc., Faraday Trans. 1* **1985**, *81*, 2235.

10.1021/la047425+ CCC: $30.25
Published on Web 03/04/2005

Table 1. Molecular Characteristics of PEO-*b*-PCL and PEO-*b*-PMCL Block Copolymers

sample PEO_x-*b*-P(M)CL_y	M_n PEO[a]	M_n PCL[b] (or PMCL)	N_A[c]	N_B[c]	EO/CL (mol %)	EO/CL (wt %)	M_w/M_n
PEO_{114}-*b*-PCL_8	5000	950	114	8	93/17	83/17	1.10
PEO_{114}-*b*-PCL_{16}	5000	1850	114	16	88/12	73/27	1.15
PEO_{114}-*b*-PCL_{19}	5000	2200	114	19	86/14	69/31	1.15
PEO_{114}-*b*-$PMCL_{12}$	5000	1500	114	12	90/10	77/23	1.12

[a] Determined by SEC with PEO standards. [b] Calculated from M_n PEO and the copolymer composition determined by ^{1}H NMR. [c] N_A and N_B: number of monomer units in the PEO and PCL blocks, respectively.

the hydrophilic block.[15,16] Depending on the relative length of the two blocks, the copolymer can form either a monolayer with the hydrophilic blocks anchored to the surface or adsorbed micelles (or a bilayer) as a result of the dominating hydrophobic interaction of the nonpolar blocks.[13,14,17−19] It may also happen that the hydrophobic blocks prefer to be in contact with the hydrophilic surface rather than to interact with the aqueous phase, leading to the formation of a polymer monolayer.

As a rule, the solution properties of the copolymer and the copolymer−surface interactions markedly influence the conformation of the adsorbed chains. For instance, PEO-*b*-PPO-*b*-PEO copolymers (where PPO stands for poly(propylene oxide)), known as Pluronics, are either nonassociated or they form micelles in water depending on the molecular structure, concentration, and temperature. The whole set of adsorbed structures can accordingly be observed at the solid surface, i.e., monolayer, micelle, and bilayer.[10,11,20]

This work is devoted to the adsorption of amphiphilic diblock copolymers from an aqueous solution onto glass and silica surfaces. These diblocks consist of a hydrophilic poly(ethylene oxide) (PEO) block associated to a hydrophobic block which can be either semicrystalline poly(ϵ-caprolactone) (PCL) or amorphous poly(γ-methyl-ϵ-caprolactone) (PMCL). These copolymers, particularly PEO-*b*-PCL, are biocompatible and partly biodegradable.[21,22] Because of the hydrophobicity of PCL,[23] organic cosolvents are usually used to dissolve these amphiphilic diblocks in water.[24−26] This is one of the reasons why their behavior at water/solid interfaces has not been extensively studied. Tanodekaew[27] studied PCL-*b*-PEO-*b*-PCL copolymers with very short (PCL) hydrophobic blocks in aqueous solution after direct dissolution in water. Vangeyte et al.[28] reported recently on the methods for the preparation of aqueous solutions of PEO-*b*-PCL copolymers.

Muller et al. studied the behavior of similar copolymers, i.e., poly(ethylene oxide)-*b*-poly(D,L-lactide) (PEO-*b*-PLA), at the surface of both hydrophilic and hydrophobic silica.[29−31] To the best of our knowledge, no report has been published on the adsorption of PEO-*b*-P(M)CL copolymers at solid surfaces.

In this study, four PEO-*b*-P(M)CL copolymers with the same PEO block (M_n = 5000) and shorter P(M)CL blocks have been studied at the silica/water or glass/water interfaces. They have been dissolved directly in water and then adsorbed on these hydrophilic surfaces. The extent of adsorption has been quantified by a total concentration depletion method and by flow microcalorimetry. The adsorbed layer has been characterized by contact angle and surface force measurements. Finally, small-angle neutron scattering (SANS) and atomic force microscopy (AFM) have been used to analyze the conformation of the chains at the hydrophilic surface.

Experimental Section

Materials. The four diblock copolymers listed in Table 1 were synthesized according to a two-step procedure detailed elsewhere.[32] Briefly, a hydroxyl-terminated poly(ethylene oxide) of M_n = 5000 (Polyscience) was used as a macroinitiator for the ring-opening polymerization of (γ-methyl)-ϵ-caprolactone. The hydroxyl end group was previously converted into an Al alkoxide, and the lactone/macroinitiator molar ratio was changed in order to control the M_n of the polyester block.

Aqueous solutions of the copolymers (0.01−1 wt %) were prepared in bidistilled water by heating at 82 °C for 12 min under vigorous stirring, followed by stirring at room temperature for 18 h before analysis.[28] For SANS experiments, a mixture of H_2O/D_2O (40/60 wt/wt) was used for matching the contrast between the solvent mixture and silica. No measurement was carried out with solutions older than 10 days.

In the case of the surface-force measurements, a 0.4 wt % stock solution in water was prepared under stirring at 80 °C for 10 min. It was then sonicated and kept at rest overnight, before use. Water was pretreated with a Millipore Milli-Q purification system, which includes a reverse osmosis unit, a mixed-bed ion exchanger, an activated carbon cartridge, and a 0.2 μm filter.

Porous silica X015 M, supplied by Biosepra (France), was used to measure the adsorption isotherms and to conduct flow microcalorimetry (FMC) and SANS experiments. According to the manufacturer, the particle size was in the 40−110 μm range, and the average pore size and specific area were 1260 Å and 31 m^2/g, respectively.

Contact angles of ethylene glycol were measured at the surface of Vel glass slides (26 × 76 mm), after rinsing of the surface with toluene, acetone, and bidistilled water, respectively, and then drying at room temperature for 24 h before use. Silicon wafers (Infineon) with a 2 nm thick native silicon oxide layer were used for AFM measurements. Prior to use, they were washed with toluene, acetone, hydrochloric acid (1 mol/L), and bidistilled water and dried for 24 h at room temperature.

(15) Mathur, S.; Moudgil, B. M. *J. Colloid Interface Sci.* **1997**, *196*, 92.
(16) Fu, Z.; Santore, M. *Macromolecules* **1998**, *31*, 7014.
(17) Grant, L. M.; Ederth, T.; Tiberg, F. *Langmuir* **2000**, *16*, 2285.
(18) Cummins, P. G.; Staples, E.; Penfold, J. *J. Phys. Chem.* **1990**, *94*, 3740.
(19) Tiberg, F.; Jönsson, B.; Lindman, B. *Langmuir* **1994**, *10*, 3714.
(20) Malmsten, M.; Linse, P.; Cosgrove, T. *Macromolecules* **1992**, *25*, 2474.
(21) Zhao, Y.; Hu, T.; Wang, S.; Wu, C. *J. Polym. Sci. Polym. Phys.* **1999**, *37*, 3288.
(22) Tjong, S. C.; Xu, Y.; Meng, Y. Z. *Polymer* **1999**, *40*, 3703.
(23) Booth, C.; Attwood, D. *Macromol. Rapid Commun.* **2000**, *21*, 501.
(24) Zhao, Y.; Liang, H.; Wang, S.; Wu, C. *J. Phys. Chem. B* **2001**, *105*, 848.
(25) Kim, S. Y.; Lee, Y. M. *Biomaterials* **2001**, *22*, 1697.
(26) Allen, C.; Maysinger, D.; Eisenberg, A. *Colloids Surf., B* **1999**, *16*, 3.
(27) Martini, L.; Attwood, D.; Collett, J. H.; Nicholas, C. V.; Tanodekaew, S.; Deng, N.; Heatley, F.; Booth, C. *J. Chem. Soc., Faraday Trans.* **1994**, *90*, 1961.
(28) Vangeyte, P.; Leyh, B.; Heinrich, M.; Grandjean, J.; Bourgaux, C.; Jérôme, R. *Langmuir* **2004**, *20*, 8442.
(29) Muller, D.; Malmsten, M.; Tanodekaew, S.; Booth, C. *J. Colloid Interface Sci.* **2000**, *228*, 317.
(30) Muller, D.; Malmsten, M.; Tanodekaew, S.; Booth, C. *J. Colloid Interface Sci.* **2000**, *228*, 326.
(31) Muller, D.; Carlsson, F.; Malmsten, M. *J. Colloid Interface Sci.* **2001**, *236*, 116.
(32) Vangeyte, P.; Jérôme, R. *J. Polym. Sci., Part A*: *Polym. Chem.* **2004**, *42*, 1132.

Bare (hydrophilic) glass was used in the surface-force experiments. The glass surface was prepared by melting one end of a borosilicate glass rod in a butane−oxygen burner until the tip formed a sphere with a diameter of approximately 4 mm. It was shown that flame-polished glass surfaces have a typical root mean square roughness of 0.10 nm,[33] which allows for the accurate measurement of interaction forces.

Methods

Adsorption Isotherms. The adsorption isotherms were measured according to the classical total concentration depletion method. One hundred milligrams of silica was dispersed in 2 mL of copolymer aqueous solutions of various concentrations and gently shaken for 48 h, which was long enough for the adsorption to reach equilibrium. The amounts of silica and copolymer solution were balanced for a large enough depletion to be measured. The silica particles were separated by sedimentation, and the PEO-*b*-P(M)CL concentration was determined by ^{1}H NMR, using a calibration curve based on the proton resonance for ethylene oxide at 3.65 ppm and methylene chloride (at 0.15 wt % constant concentration) at 5.3 ppm. The relaxation delay between pulses was 5 s, i.e., five times longer than T_1.

Flow Microcalorimetry (FMC). Adsorption experiments were performed with a Microscal flow microcalorimeter, equipped with a calorimetric cell (0.17 mL volume) and a downstream refractometer as detailed by Groszek.[34] The cell was filled with 0.06 g (accurately weighed) of silica and eluted with either water or a block copolymer solution of known concentration at a constant flow rate of 3 mL/h. Heat exchanges in the cell were detected by two adjacent thermistors and recorded as a function of time. The peak area was proportional to the total heat released or absorbed and compared to a reference peak recorded under similar conditions as a result of a known current flowing through a resistance. The experimental adsorption heat was reproducible with a standard deviation of ∼5%.

Because the preadsorbed solvent was displaced by the flowing copolymer solution, the enthalpy of displacement was measured rather than the enthalpy of adsorption.[35] The heat of displacement, ΔH^{dis}, was calculated from the experimental calorimetric peak, Q, according to eq 1

$$\Delta H^{dis} = Q - \Delta H^{dil} \quad (1)$$

where ΔH^{dil} is the dilution enthalpy, which was determined by flowing the copolymer solution (blank experiment) through the cell filled with Teflon (poly(tetrafluoroethylene)) rather than with silica (Figure 3, bottom).

The amount of compound adsorbed onto silica was calculated as follows. The concentration of the effluent was monitored as a function of time by the downstream refractive index detector. The same experiment was repeated with the cell filled with Teflon instead of silica. Because of the very low surface area (0.1 m^2/g) of Teflon and its low affinity for hydrocarbons, it was assumed that the copolymer was not adsorbed at all. The amount of solute retained on silica was then calculated from the difference between the refractive index signals in the two experiments (Figure 3, top).

Contact Angle. The contact angle of ethylene glycol was measured on precoated glass. Water was not used because of the possible solubilization of the adsorbed copolymer. Ethylene glycol has a polar component of surface energy (21.3 mN/m) lower than that of water (46.8 mN/m), and its viscosity at ambient conditions facilitates drop formation and deposition. The experimental device consisted of a camera (Electronic Shutter C 800) for the capture of the drop image and software (PC-scope Scene Version 1.01) for the calculation of the contact angle from the height and diameter of the drop. The glass slides were coated by immersing them (for 1 or 48 h) in concentrated (0.6 wt %) or diluted (0.015 wt %) copolymer solutions using water (for PEO and PEO-*b*-PCL) or toluene (for PCL) as a solvent. The slides were finally dried and stored at room temperature. The values reported for contact angles were the average of at least 20 measurements.

Surface Interaction Forces. Forces were measured with a noninterferometric surface-force apparatus known as MASIF.[36] A bimorph force/deflection sensor measured interaction forces versus surface separation between two spherical surfaces. One of the surfaces (the bottom surface) was mounted on the tip of the bimorph and the other one (the upper surface) on a piezoelectric tube. The assembly was placed in a stainless steel cell of ∼10 mL and mounted on a translation stage isolated from electrical and sound noise. In a typical force measurement, the upper surface was driven by applying a triangular voltage wave to the piezo crystal. The charge triggered by any deflection of the bimorph (that held the lower surface), as a result of repulsive or attractive forces, was recorded simultaneously. Once the surfaces came into hard-wall contact, the motion of the piezo directly deflected the bimorph allowing the force sensor to be calibrated against the known piezo crystal expansion (and contraction) as measured by a linear variable differential transformer (LVDT). From the deflection and the spring constant of the bimorph, the data were converted into force−distance curves by application of Hooke's law. It must be noted that the noninterferometric surface-force apparatus was not suited to the absolute determination of the zero surface separation and thus of the layer thickness. The distance reported in the figures was calculated from the hard wall contact.

The normal radii of curvature (r_1 and r_2) for each surface were measured at the end of the experiment with a micrometer, and the local harmonic mean radius of interaction, R, was calculated as $R = 2r_1r_2/(r_1 + r_2)$. The spring constant of the bimorph (typically 100 N/m) was also determined at the end of each experiment from the deflection produced by placing known weights on the sensor. The force (F) was normalized by the harmonic mean radius of the surfaces (F/R).

The measurement chamber was assembled, and the solutions were prepared in a laminar flow cabinet. Before each series of experiments, the interaction profiles were determined in air to ensure that the system was free from contamination. Water was then added into the chamber, and the interaction profile was recorded. A concentrated stock polymer solution was then added until the desired concentration in the chamber was attained. To change the polymer concentration, part of the volume of the chamber was drained and replaced by a polymer solution of appropriate composition. Therefore, each solution was in contact with a surface preequilibrated with the previous (more diluted) solution rather than with a bare surface.

In some cases, the experimental forces were analyzed by the classical Derjaguin−Landau−Verwey−Overbeek theory,[37,38] taking into account the double-layer and

(33) Ederth, T.; Claesson, P. M.; Lindberg, B. *Langmuir* **1998**, *14*, 4782.
(34) Groszek, A. J. *Thermochim. Acta* **1998**, *312*, 133.
(35) Rouquerol, J. *Pure Appl. Chem.* **1985**, *57*, 69.
(36) Parker, J. L.; Claesson, P. M. *Langmuir* **1994**, *10*, 635.
(37) Dejarguin, B.; Landau, L. *Acta Physiochem.* **1941**, *14*, 633.

attractive van der Waals forces. The double-layer force was calculated according to the nonlinear Poisson−Boltzmann model, under conditions of constant surface charge boundary, which usually provides a better approximation of the measured forces than those calculated under constant potential boundary conditions. The van der Waals forces between the block-copolymer-coated interfaces were estimated on the basis of a three-layer (surface−polymer layer−solvent) model.[39]

Small-Angle Neutron Scattering (SANS). SANS experiments were performed at the FRJ-2 reactor (Forschungszentrum Jülich, Germany) using the KWS-1 instrument and at the Orphée reactor of the Laboratoire Léon Brillouin (Saclay, France) with the PACE instrument. The samples were kept in quartz cells of 1 mm (KWS-1) or 2 mm (PACE) path length.

Samples were prepared in the same way as for the measurement of the adsorption isotherms. After silica was mixed with the copolymer solution, the supernatant was eliminated, and the silica particles were rinsed two times with the solvent in order to eliminate the interstitial copolymer solution.

The KWS-1 small-angle spectrometer was equipped with a two-dimensional area detector of 60 × 60 cm^2 with a space resolution of 0.8 × 0.8 cm^2. The neutron wavelength, λ, was set at 7 Å with a resolution ($\Delta\lambda/\lambda$) of 20%. The beam cross section was 6 × 6 mm^2. The measurements were performed at two sample-to-detector distances (8 and 2 m) corresponding to the scattering vector (q) ranges of 0.006−0.04 and 0.024−0.15 Å^{-1}, respectively. Radial averaging led to a one-dimensional scattering function $I(q)$. Measurements on the PACE instrument were performed at a neutron wavelength of 5 Å, with a resolution of 10%, a beam diameter of 10 mm, and a range of scattering vector, q, extending from 0.004 to 0.044 Å^{-1} (sample−detector distance of 4.7 m) and from 0.014 to 0.15 Å^{-1} (distance of 2.8 m). The data were collected with a two-dimensional area detector made of 30 concentric rings of 1 cm width.

Parasitic contributions of the electronic and ambient background and the sample holder were eliminated by standard data handling procedures. The scattering intensities were converted to macroscopic scattering cross sections per unit volume, $d\Sigma/d\Omega$ (unit: length^{-1}), based on a calibration with either low-density polyethylene (LUPOLEN) (KWS-1) or the incoherent scattering of water (PACE). The polymer contribution to the scattering cross section was determined by subtracting the cross section for wet bare silica, weighted by its volume fraction.

Whenever the inverse (q^{-1}) of the scattering vector is small compared to the radius of curvature of the solid−liquid interface, the latter is considered as flat at this q scale (Porod's condition). Because the largest q^{-1} value sampled in the experiments, $q^{-1} = (0.004\ \text{Å}^{-1})^{-1} = 250$ Å, was much smaller than the typical silica dimensions (particle diameter of 40−110 μm and pore size of 1260 Å), the condition for this approximation was fulfilled. Moreover, the interface was randomly oriented with respect to the scattering vector.

For an isotropic and incompressible three-component system (polymer/solid/solvent), the macroscopic cross section per sample unit volume, $d\Sigma/d\Omega$ is given by eq 2[40]

$$\frac{d\Sigma}{d\Omega}(q) = (n_p - n_s)^2 S_{pp}(q) + (n_g - n_s)^2 S_{gg}(q) + 2(n_p - n_s)(n_g - n_s) S_{pg}(q) \quad (2)$$

where n_p, n_g, and n_s, are the scattering length densities of the scattering units of the polymer (p), the solid grain (g), and the solvent (s), respectively. The three partial structure factors correspond to the polymer−polymer (S_{pp}), polymer−solid (S_{pg}), and solid−solid (S_{gg}) correlations. The contrast of silica (n_g) and the solvent (n_s) was matched by using a 60/40 wt/wt D_2O/H_2O mixture.[41] Equation 2 was then reduced to

$$\frac{d\Sigma}{d\Omega}(q) = (n_p - n_s)^2 S_{pp}(q) \quad (3)$$

The coherent scattering cross section then depended only on the characteristics of the layer adsorbed at the interface (adsorbed mass per surface unit, layer thickness, and structure) and on the specific interfacial area, S/V (S is the total surface area at the solid/liquid interface and V is the sample volume). As reported in the results and discussion section, different adsorption models were confronted with the experimental data.

Atomic Force Microscopy (AFM). AFM experiments were carried out with a Nanoscope III microscope (Digital Instrument Inc.) operated in air at room temperature in the Tapping Mode. The instrument with the Extender Electronics Module provided height and phase images simultaneously. Samples were prepared by dipping the silicon wafer in a copolymer aqueous solution of appropriate concentration (0.7 or 0.015 wt %) for 2 h. The excess solution was eliminated by gravity drainage, followed by washing with a small amount of bidistilled water and drying at room temperature for 24 h.

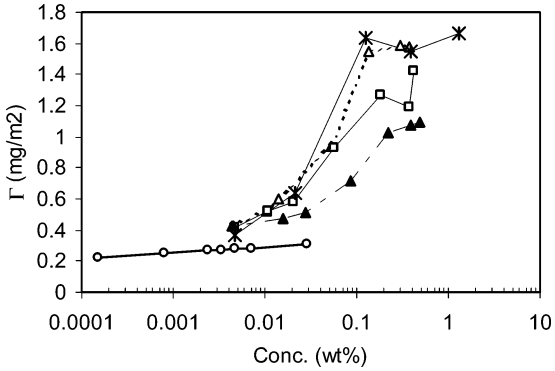

Figure 1. Adsorption isotherms for the PEO_{114}-*b*-PCL_8 (▲), PEO_{114}-*b*-PCL_{16} (∗), PEO_{114}-*b*-PCL_{19} (△), and PEO_{114}-*b*-$PMCL_{12}$ (□) copolymers and PEO (○) on silica, as measured by the concentration depletion method (lines are a guide for eyes).

Results and Discussion

Adsorption of PEO-*b*-P(M)CL. Figure 1 compares the adsorption isotherms for homoPEO and the PEO-*b*-P(M)CL copolymers under investigation (Table 1) on hydrophilic silica, as measured by the total concentration depletion method. PEO (M_n = 5000) exhibits a high adsorption affinity with a plateau value of ∼0.31 mg/m^2, in good agreement with reported data.[42−44] This observation validates the experimental method.

(38) Verwey, E. G. W.; Overbeek, J. T. G. *The Theory of the Stability of Liophobic Colloids*; Elsevier: Amsterdam, 1948.
(39) Ninham, B. W.; Parsegian, V. A. *J. Chem. Phys.* **1970**, *52*, 4578.
(40) Auvray, L. *Scattering by Polymers at Interfaces*, In *Neutron, X-ray and Light Scattering*; Lindner, P., Zemb, T., Eds.; North-Holland: Amsterdam, 1991.
(41) Merzbacher, C. I.; Barker, J. G.; Swider, K. E.; Rolison, D. R. *J. Non-Cryst. Solids* **1998**, *224*, 92.
(42) Dijt, J. C.; Cohen Stuart, M. A.; Fleer, G. J. *Macromolecules* **1994**, *27*, 3219.
(43) Linse, P.; Hatton, T. A. *Langmuir* **1997**, *13*, 4066.
(44) Rippner, B.; Boschkova, K.; Claesson, P. M.; Arnebrant, T. *Langmuir* **2002**, *18*, 5213.

Table 2. cmc in Water and Adsorption Properties of PEO and PEO_x-*b*-P(M)CL_y Copolymers at the Hydrophilic Silica−Water Interface

sample	cmc[a] (wt %)	C_c[b] (wt %)	Γ_{max} (AI) (mg/m^2)	Γ_{max} (FMC) (mg/m^2)
PEO_{114}			0.31	0.35
PEO_{114}-*b*-PCL_8	0.0045	0.078	1.09	1.19
PEO_{114}-*b*-PCL_{16}	0.0015	0.022	1.63	
PEO_{114}-*b*-PCL_{19}	0.0011	0.026	1.58	1.65
PEO_{114}-*b*-$PMCL_{12}$	0.0023	0.042	1.42	

[a] From ref 28. [b] Concentration at which the cooperative adsorption occurs, as determined from the adsorption isotherms (AI).

The adsorbed amount is higher for the PEO-*b*-P(M)CL copolymers than for PEO of similar molecular weight. Moreover, the maximum adsorption increases with the hydrophobic block length, which indicates that this block plays an important role in the adsorption mechanism.

The adsorption isotherm of PEO is typical of the high affinity type, i.e., a high adsorbed amount even at low concentrations. In contrast, the shape of the adsorption isotherms for the block copolymers is sigmoidal, which is indicative of a cooperative adsorption mechanism. Quite comparable adsorption isotherms were reported for PEO-containing surfactants of low molecular weight on silica.[45] At a critical concentration, usually lower than the bulk critical micelle concentration (cmc), these surfactants are commonly adsorbed cooperatively as micelles at the interface and the adsorbed amount levels off at the cmc.[46] A similar behavior was reported for block copolymers,[29,30] although there is no clear relationship between the bulk cmc and the onset of the cooperative adsorption at the interface.

Eskilsson et al.[12] studied the adsorption of triblock copolymers of PEO and polytetrahydrofuran (PTHF) (PEO-*b*-PTHF-*b*-PEO) on hydrophilic silica. The onset of cooperative adsorption occurs at a concentration approximately 2 orders of magnitude lower than the bulk cmc. The lower aggregation number at the interface compared to micelles in the bulk solution suggests a preferential interface-induced micellization prior to the usual bulk micellization. Muller et al.[29] studied the adsorption of PEO-*b*-PLA on hydrophilic silica and a cooperative adsorption process was reported, although at concentrations exceeding the cmc. The experimental results were not consistent for copolymers of different molecular weights, such that no direct correlation between adsorption and bulk micellization could be drawn.

In this work, the cooperative adsorption (Figure 1) starts at a concentration higher than the cmc estimated from surface tension measurements.[28] Table 2 compares the cooperative adsorption concentration (C_c) and the bulk micellization concentration (cmc). Figure 1 shows that the cooperative adsorption regime occurs over a large concentration range, similarly to the broad discontinuity in the surface tension data at the cmc. This observation is probably related to a polydispersity effect and the faster depletion of the more surface active components from the bulk solution.[43] Therefore, the cmc for block copolymers may be underestimated when extracted from surface tension measurements.[44] Direct comparison of the onset of bulk micellization and cooperative binding to the solid surfaces is thus unreliable.

The amounts of PEO_{114}-*b*-PCL_{19} and PEO_{114}-*b*-PCL_8 copolymers adsorbed on silica upon increasing concentration in solution were determined by flow microcalorimetry (Figure 2). Even though the shape of the adsorption isotherms measured by FMC and by the total depletion method (Figure 1) is not the same (static vs dynamic methods), the maximum adsorbed amount is similar in the two cases (Table 2).

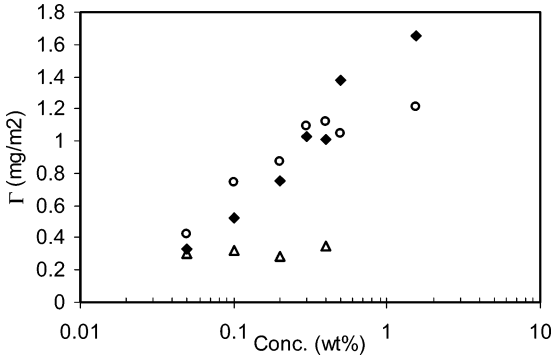

Figure 2. Adsorbed amount of PEO_{114}-*b*-PCL_8 (○), PEO_{114}-*b*-PCL_{19} (◆), and PEO (△) on hydrophilic silica as a function of concentration in water, measured by FMC at a flow rate of 3 mL/h.

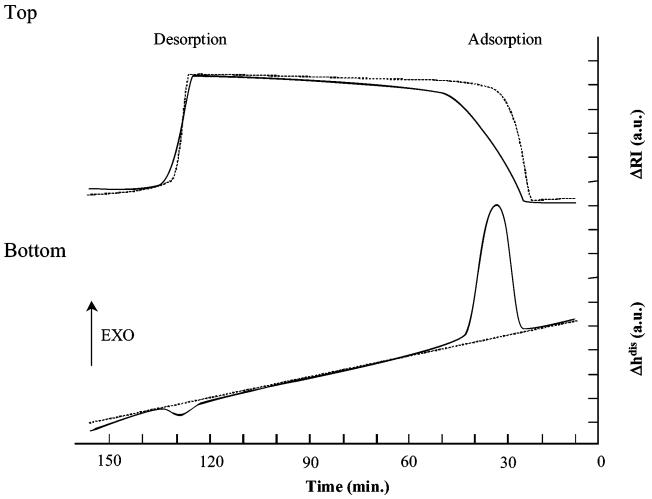

Figure 3. Simultaneous record of the heat exchanged on adsorption (bottom) on silica (full line) and Teflon (dashed line) and the amount of PEO_{114}-*b*-PCL_{19} copolymer adsorbed by FMC (top) from a 0.3 wt % PEO_{114}-*b*-PCL_{19} aqueous solution on at 25 °C. Flow rate = 3 mL/h.

The heat exchange upon adsorption was measured for both silica and Teflon. Figure 3 shows that the adsorption of PEO-*b*-PCL block copolymers is exothermic on silica, whereas no heat is exchanged when Teflon is substituted for silica, which indicates that the copolymer adsorption on Teflon and ΔH^{dil} (dilution enthalpy variation) are negligible. The heat exchanged upon adsorption of PEO_{114}-*b*-PCL_{19}, PEO_{114}-*b*-PCL_8, and PEO was measured as a function of their concentration. A small increase is observed from ~10 to ~13 mJ/m^2 with increased concentration from 0.2 to 1.5 wt %. Below 0.2 wt %, the experimental data fluctuate as a result of slow adsorption which makes determination of the end of the adsorption peak difficult. Experiments were also conducted for copolymers at a constant concentration (0.3 wt %) as a function of the hydrophobic block length. This structural parameter has no significant effect on ΔH^{dis}, at least in the investigated range (M_n PCL < 2500). This observation indicates that the hydrophobic PCL block does not interact directly with silica at this copolymer concentration.

Elution of the adsorbed copolymer with pure water shows a very weak endothermic (desorption) peak (~0.2

(45) Levitz, P. *Langmuir* **1991**, *7*, 1595.
(46) Clunie, J. S.; Ingram, B. T. Adsorption of Nonionic Surfactants. In *Adsorption from Solution at the Solid/Liquid Interface*; Parfitt, G. D., Rochester, C. H., Eds.; Academic Press: London, 1983; Chapter 3.

Table 3. Contact Angles of Ethylene Glycol at the Silica Surface after Adsorption of PEO, PCL, and PEO_x-*b*-PCL_y Copolymers

incubation time (h)	concn (wt %)	contact angles (deg)				
		silica	PEO	PCL	PEO_{114}-*b*-PCL_{19}	PEO_{114}-*b*-PCL_8
48	0.6	15.0 ± 2.0	30.8 ± 3.8	52.4 ± 3.2	28.9 ± 4.1	33.2 ± 4.6
	0.015				40.2 ± 5.1	
1	0.6		30.1 ± 3.6	55 ± 4.2	37.3 ± 3.3	36.7 ± 5.6

mJ/m^2) (Figure 3, bottom), and the refractometric measurements indicate that a very small amount of copolymer is actually desorbed. The copolymer adsorption is thus basically irreversible.[47]

Surface Behavior. The contact angle of ethylene glycol was measured at the surface of glass slides previously dipped in aqueous solutions of PEO_{114}-*b*-PCL_{19} and PEO_{114}-*b*-PCL_8, with a 0.015 and 0.6 wt % concentration, for either 1 or 48 h. AFM images of the surface (vide infra) confirmed that a copolymer layer was deposited on the glass slide after dipping and drying.

The data reported in Table 3 show that the contact angles measured for films deposited from high concentration solutions (0.6 wt %) are independent of the adsorption time (the differences are in the limits of the experimental error) except for the diblock polymer with the higher PCL content. As a rule, the contact angles for the two diblocks are very close to that of PEO at long equilibration time. This indicates that PCL is buried within the film. However, when the M_n of the PCL block is higher, it seems that at least part of PCL is initially exposed to water and that it takes time for it to reorganize beneath the surface.

At low surface coverage (adsorption from dilute copolymer solution), the contact angle for the PEO_{114}-*b*-PCL_{19} copolymer is much higher even for a long dipping period of time. At this concentration (lower than C_c), the copolymer forms micelles in equilibrium with free chains. Upon adsorption, the nonassociated copolymer chains are also adsorbed in such a way that PCL chains contribute to the contact angle, which accordingly is higher than that of PEO (and bare silica surfaces). Although the PCL chains strive to avoid contact with water, they do not want to interact with silica, as shown by FMC. Therefore, these hydrophobic chains have to adopt a conformation such that they minimize their presence at the two interfaces as extensively as possible.

Surface-force measurements were performed first with bare glass surfaces. The interaction forces between two bare glass surfaces across water is shown in Figure 4. The force−distance relationship fits the DLVO profile down to a separation of ca. 5 nm. At shorter separation distances, extra repulsion forces dominate. Short-range repulsive forces between glass or silica surfaces in aqueous solution have been reported previously[48,49] and rationalized in terms of dehydration of polar silanol groups (hydration forces)[50] or compression of short polysialic acid chains (steric repulsion).[48] The apparent surface potential at large separation distances and the area per surface charge extracted from the curve fitting on the assumption of constant surface charge boundary conditions are −71 mV (1.85×10^{-3} C/m^2) and 86.5 nm^2, respectively.

Figure 5 shows that the addition of PEO_{114}-*b*-PCL_{19} up to concentration of 0.01 wt % results in a remarkable change in the surface-force profile. The long-range double-layer repulsive force observed in the case of the bare surfaces is replaced by repulsive steric interactions. Furthermore, the force profile on retraction shows a moderately strong adhesion that was originally absent. This observation confirms that adsorption occurs at this low polymer concentration in agreement with the adsorption isotherm shown in Figure 1. It must be noted that upon separation, the force profile does not show the typical jump out of contact. This situation occurs when the applied negative force exceeds the adhesion force and the force gradient exceeds the spring constant. In the present case, the attractive forces decay gradually up to an apparent surface separation of approximately 80−100 nm. Despite

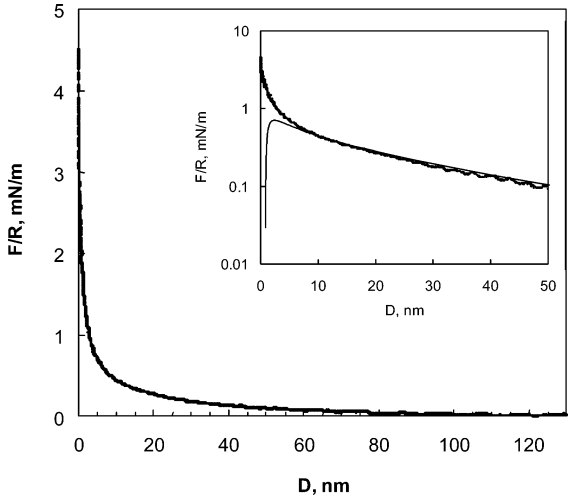

Figure 4. Interaction force normalized by the radius as a function of the separation distance of glass spheres across water. The inward and outward runs overlap. A semilogarithmic plot is shown in the inset, with a DLVO fitting with an apparent surface potential $\Psi_0 = -71$ mV, a Debye length $\kappa^{-1} = 37$ nm and a Hamaker constant $A = 0.7 \times 10^{-20}$ J. Data are collected with the bimorph surface force apparatus (MASIF) at 22 °C.

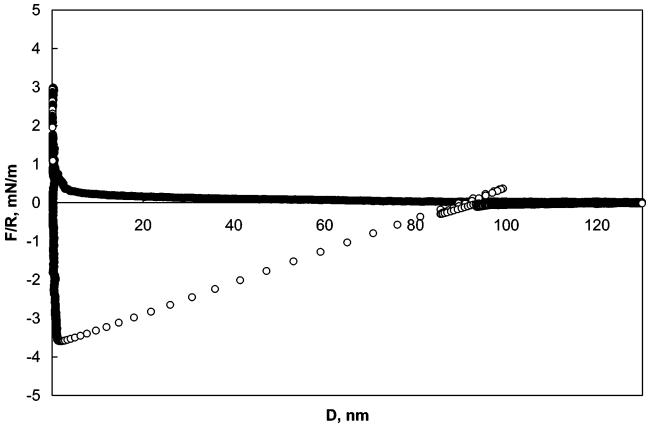

Figure 5. Force normalized by the radius as a function of the separation distance of glass spheres across 0.01 wt % PEO_{114}-*b*-PCL_{19} aqueous solution. The filled black circles curve is the approach curve and the open circles curve is the separation (outward) one after equilibrium. The data were collected with the bimorph surface force apparatus (MASIF) at 22 °C.

(47) Cohen Stuart, M. A.; Fleer, G. J.; Scheutjens, J. M. H. M. *J. Colloid Interface Sci.* **1984**, *97*, 515.
(48) Vigil, G.; Xu, Z.; Steinberg, S.; Israelachvili, J. *J. Colloid Interface Sci.* **1994**, *165*, 367.
(49) Yaminsky, V. V.; Ninham, B. W.; Pashley, R. M. *Langmuir* **1998**, *14*, 3223.
(50) Chapel, J. P. *Langmuir* **1994**, *10*, 4237.

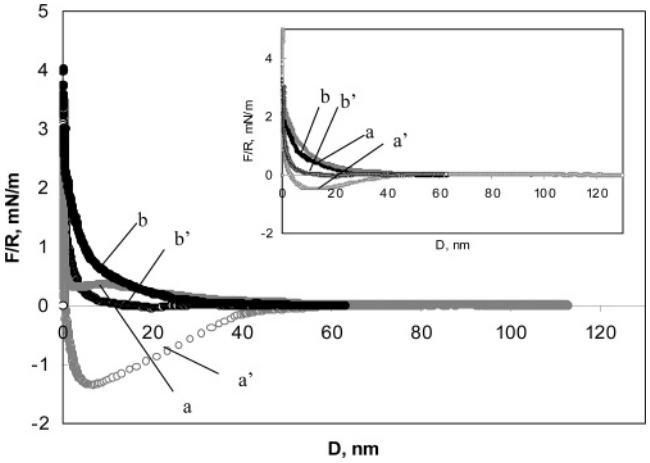

Figure 6. Force normalized by the radius as a function of the separation distance of glass spheres across 0.1 wt % PEO_{114}-*b*-PCL_{19} aqueous solution. The filled gray circles curve (a) is the approach curve after 5 h of incubation and the gray open circles curve (a′) is the separation (outward) one. In both cases the driving rate was 18 nm/s. The black circles curves are the force profiles after 22 h of equilibration. The filled (b) and the open symbols (b′) correspond to the inward and outward runs, respectively. The driving rate was 6 nm/s. Inset: comparison of force after 22 h of equilibration recorded at a driving rate of 6 and 56 nm/s, (b, b′) and (a, a′), respectively. The data were collected with the bimorph surface force apparatus (MASIF) at 22 °C.

the fact that during the approach no polymer bridging takes place, it appears that after the surfaces reach contact, polymer chains interpenetrate the adsorbed layers of both surfaces. As a result, polymer bridging is established, and the adhesion observed during retraction of the surfaces involves the gradual unfolding and extension of polymer chains.

It must be noted that the adhesion force is higher than that between PEO-coated surfaces[51] and significantly smaller than that between nonpolar surfaces.[52] This observation is consistent with the contact angle data reported at low polymer concentrations.

Figure 6 shows the interaction force profile at the higher polymer concentration of 0.1 wt %. The long-range force profile on approach monitored after 2−5 h of equilibration is comparable to the one measured at the lower polymer concentration. However, a lower repulsive force is observed at short distances, which indicates that the layer structure partially collapses as the surfaces are forced together. Finally, a strong repulsion is observed at very short distances. On retraction, the adhesion is noticeably lower than at the 0.01 wt % concentration. In reference to the previous explanation for the origin of the adhesion, it might be concluded that the partial availability of PCL at the surface after 5 h of incubation (see contact angle data in Table 3) is a plausible explanation. The hydrophobic interaction and layer entanglements can account for the layer structure relaxation during separation, as strongly suggested by the fact that the surfaces come apart at a finite distance with respect to the hard wall contact (this was not the case at the lower polymer concentration).

After equilibrium adsorption, i.e., after more than 22 h of incubation, the force profile changes significantly. Both the layers collapse on approach and the adhesion observed under decompression disappears, which is indicative of slow structural changes in the adsorbed layer, more likely leading to a surface layer of PEO in contact with water. It should be noted that the same behavior was observed at different contact areas after the incubation time, which rules out possible effects due to experimental conditions or the way the surfaces were probed. The interaction profile depends on the rate of approach and separation as illustrated in the inset of Figure 6. When the driving rate is increased from 6 to 56 nm/s, increased repulsion upon compression and adhesion upon separation are noted, consistent with more important hydrodynamic interactions at higher driving rates.

No sudden change in the force profile is observed either upon approach or retraction, which supports that the polymer layer remains adsorbed as is the case for a densely packed adsorbed layer.

Substitution of water and later of a NaCl solution (up to 10 mM concentration) for the polymer solution does not significantly change the force profile, which also suggests that no desorption occurs, as was observed by FMC. This observation is in contrast to the adsorption of diblock copolymers of PEO and polylactide on hydrophilic silica,[29] which were partially desorbed under similar conditions.

Structure of the Adsorbed Layer. *SANS Experimental Data and Layer Models*. Small-angle neutron scattering experiments were performed with the copolymers adsorbed on hydrophilic silica, at the saturation regime (i.e., concentration at the maximum of the adsorption isotherms) and the half-saturation regime (i.e., concentration at the onset of the cooperative adsorption).

In the Porod's regime, the scattered intensity depends on the concentration profile in the direction perpendicular to the interface, $\phi(z)$, and on the concentration fluctuations within the adsorbed layer in the directions parallel to the interface (x and y directions).[40,53] However, if the average distance between two adjacent adsorbed chains is small compared to $2\pi/q$, the layer can be considered as homogeneous along x and y, so that the scattering cross section is governed by $\phi(z)$ only. On the basis of the depletion method measurements, adsorbed quantities lie in the 1−1.6 mg/m^2 range. In the case of single chain adsorption, the average interchain distance within the (x,y) plane, a, is smaller than 30 Å. Correlation within the plane is thus expected to be observed for $q > 2\pi/30 = 0.2$ Å^{-1}, i.e., above the q range sampled. Analytical models assuming different concentration profiles, $\phi(z)$, have been confronted with the experimental data. The adsorbed copolymer has been modeled by two superimposed sublayers: a homogeneous dense hydrophobic layer in contact with the silica interface, covered by a hydrophilic layer with three possible concentration profiles: (i) a homogeneous step concentration profile (Figure 7a); (ii) a homogeneous parabolic concentration profile (Figure 7b); (iii) Gaussian chains anchored to the hydrophobic layer and spread according to a square bidimensional network all over the surface (Figure 7c). The standard way to derive the scattering cross section for such models can be found, e.g., in ref 40.

According to Auvray et al.,[40,53] plotting the data as $q^2I(q)$ vs q is a useful representation. However, the three models are unable to account for the maximum observed in the low q range (around $q = 0.03$ Å^{-1}), as illustrated by the fit of the model based on Gaussian chains anchored to the hydrophobic layer to the experimental data for the PEO_{114}-*b*-PCL_{19} copolymer (Figure 8). Therefore, models based on the superposition of homogeneous sublayers have to be disregarded at least for the experimental conditions of this work. With reference to the contact angle and MASIF

(51) Claesson, P. M.; Gölander, C. G. *J. Colloid Interface Sci.* **1987**, *117*, 366.
(52) Claesson, P. M.; Blom, C. E.; Herder, P. C.; Ninham, B. W. *J. Colloid Interface Sci.* **1986**, *114*, 234.
(53) Auroy, P.; Auvray, L.; Leger, L. *Macromolecules* **1991**, *24*, 2523.

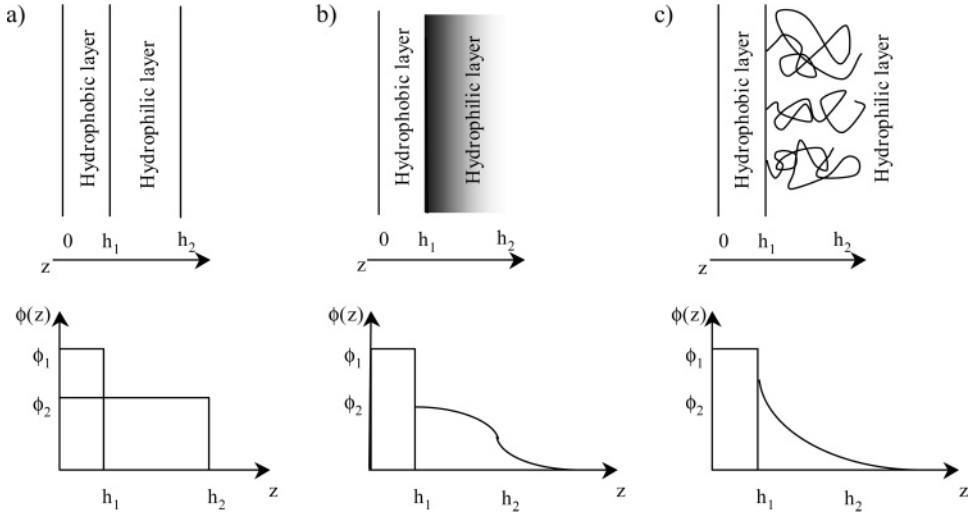

Figure 7. Models for the analysis of the scattering cross sections in SANS experiments. Each model is based on a dense homogeneous hydrophobic inner layer and a hydrophilic layer described by three possible profiles: (a) homogeneous layer; (b) parabolic profile; (c) Gaussian chains.

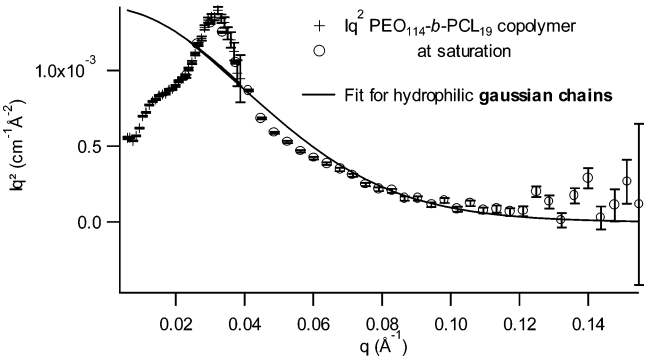

Figure 8. Fit of the model C (Figure 7) to the experimental data for the PEO_{114}-*b*-PCL_{19} copolymer (under surface saturation conditions).

data, a three-layer organization might be considered with PEO at the interfaces with silica and water, respectively, and an inner PCL layer. This model also fails to fit the $q^2I(q)$ plot in the 0.03 $Å^{-1}$ region. A common feature of all the tested models is that only the concentration profile in the z direction is taken into account. Thus, correlations within the adsorbed layer in the (x,y) plane must be considered in the modeling. Data at relatively low q values point rather to the adsorption of nanoscale self-assembled structures. PEO-*b*-PCL copolymers form micelles in aqueous solution with an average aggregation number in the 50−120 range.[28] On the assumption that micelles are adsorbed, an average intermicellar distance, d, of 200−300 Å can be estimated from the adsorbed masses. The intermicellar correlations are then expected to trigger a maximum at $q \approx 2\pi/d = 0.02-0.03$ $Å^{-1}$. The next subsection deals with a theoretical model for adsorbed micelles.

Adsorption of Self-Assembled Species. Figure 9 is a schematic view of spherical PEO-*b*-P(M)CL copolymer micelles adsorbed at the silica−water interface. These micelles consist of a dense core of hydrophobic polycaprolactone (with radius R), surrounded by a corona of swollen hydrophilic poly(ethylene oxide) blocks described as rigid rods of length L. According to a previous study of the same copolymers in water, the so-called core−rods model allowed fitting of the scattering data.[28] The micelles are assumed to form a liquidlike two-dimensional monolayer, with the minimum distance between the micelle centers equal to σ.

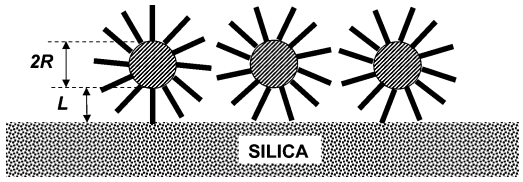

Figure 9. Micellar model used for the analysis of the SANS macroscopic cross section. Spherically symmetric micelles are assumed, consisting of a dense hydrophobic PCL core (radius $= R$) surrounded by rodlike PEO chains of an effective length L.

The orientation-averaged macroscopic scattering cross section per sample unit volume is given by eq 4, in Porod's regime and under conditions of contrast matching between silica and solvent (more information is provided in the "Supporting Information"). It is the sum of two contributions: the profile term, $\bar{I}_{pp}(q)$, related to the concentration profile in the direction perpendicular to the surface, and the correlation term, $\tilde{I}_{pp}(q)$, governed by the two-dimensional organization within the layer of adsorbed micelles.

$$\frac{d\Sigma}{d\Omega}(q) = \bar{I}_{pp}(q) + \tilde{I}_{pp}(q) \tag{4}$$

The profile term is expressed by eq 5

$$\bar{I}_{pp}(q) = 2\pi \frac{S}{V}\left(\frac{\Gamma}{\bar{M}}\right)^2\left[\frac{\bar{M}_1}{d_1}(n_1 - n_s) + \frac{\bar{M}_2}{d_2}(n_2 - n_s)\right]^2 \frac{P(q)}{q^2} \tag{5}$$

$P(q)$ is the form factor of the single micelles, normalized to 1 at $q = 0$.

On the basis of a mean-field hard sphere potential approximation for the micellar two-dimensional pair correlation function, the correlation term can be expressed by eq 6

$$\tilde{I}_{pp}(q) = \frac{\pi\sigma^2}{2}\frac{S}{V}\left(\frac{\Gamma}{\bar{M}}\right)^2\left[\frac{\bar{M}_1}{d_1}(n_1 - n_s) + \frac{\bar{M}_2}{d_2}(n_2 - n_s)\right]^2 P(q) \int_0^{\pi} d\theta \sin\theta\left[1 - 2\pi\frac{N_{mic}}{S}\int_0^{\sigma} d\rho\rho J_0(q\rho \sin\theta)\right] \tag{6}$$

$J_0(x)$ is the zero-order Bessel function. N_{mic}/S is the number of micelles adsorbed per unit surface. The indices 1 and 2 refer to the hydrophobic and hydrophilic blocks, respectively. Γ is the adsorbed copolymer mass per unit surface. $\bar{M}$, $\bar{M}_1$, and $\bar{M}_2$ are the molar masses of the copolymer, the hydrophobic block, and the hydrophilic block, respectively. d_i is the density and n_i the scattering length density of the block i.

The form factor for the core−rigid rods model is given by eq 7[28]

$$P(q) = \alpha_1^2\left\{\frac{3}{(qR)^3}[\sin(qR) - (qR)\cos(qR)]\right\}^2 + \frac{\alpha_2^2}{N_{agg}}\left\{\frac{2}{qL}Si(qL) - \frac{\sin^2\left(\frac{qL}{2}\right)}{\left(\frac{qL}{2}\right)^2}\right\} + 2\alpha_1\alpha_2\frac{3[\sin(qR) - (qR)\cos(qR)]}{(qR)^3}\frac{Si[q(R+L)] - Si(qR)}{qL} + \frac{\alpha_2^2}{N_{agg}}(N_{agg} - 1)\left\{\frac{Si[q(R+L)] - Si(qR)}{qL}\right\}^2 \quad (7)$$

where

$$Si(x) = \int_0^x \frac{\sin x'}{x'}\,dx'$$

$$\alpha_1 = \frac{z_1\tilde{b}_1}{z_1\tilde{b}_1 + z_2\tilde{b}_2}$$

and

$$\alpha_2 = \frac{z_2\tilde{b}_2}{z_1\tilde{b}_1 + z_2\tilde{b}_2}$$

z_1 and z_2 are the polymerization degrees of the hydrophobic and hydrophilic blocks, respectively. The excess scattering lengths of the scatterers are denoted as $\tilde{b}_1$ and $\tilde{b}_2$. N_{agg} is the aggregation number.

At $q = 0$, eqs 4−7 are reduced to

$$\lim_{q\to 0} q^2\frac{d\Sigma}{d\Omega} = 2\pi\frac{S}{V}\left(\frac{\Gamma}{\bar{M}}\right)^2\left[\frac{\bar{M}_1}{d_1}(n_1 - n_s) + \frac{\bar{M}_2}{d_2}(n_2 - n_s)\right]^2 \quad (8)$$

The scattering intensity at $q = 0$ is expectedly determined by the adsorbed copolymer amount, thus a macroscopic quantity.

There are four unknown parameters in eqs 5−7: the adsorbed amount of copolymer, Γ, the intermicellar distance, σ, and the structural parameters of the micelles (R and L) which govern the form factor $P(q)$. Although these parameters can be determined by fitting eq 4 to the experimental data taking eqs 5−7 into account, a simplified approach was used first. At $q \le 0.04$ Å^{-1}, the micellar form factor was approximated by Guinier's equation, in relation to the radius of gyration of the micelles, R_g[54]

$$P(q) = \exp\left(\frac{-q^2R_g^2}{3}\right) \quad (9)$$

χ^2, i.e., the sum of the squares of the differences between the experimental and fitted intensities, was minimized by combining R_g, σ, and Γ adequately. In a second step, the full q range was considered, and the form factor was approximated by a core−rods model (eq 7). The χ^2 criterion was also used to extract the best combination of R, L, σ, and Γ. In both cases, no black-box fitting algorithm was used. To make sure that the global minimum of the χ^2 hypersurface was found, the latter was mapped systematically as a function of the different parameters. A first coarse investigation was followed by a finer mesh inspection. A moderate micellar size polydispersity was introduced using a Gaussian distribution for the core radius with a standard deviation of 0.5 nm, as in ref 28.

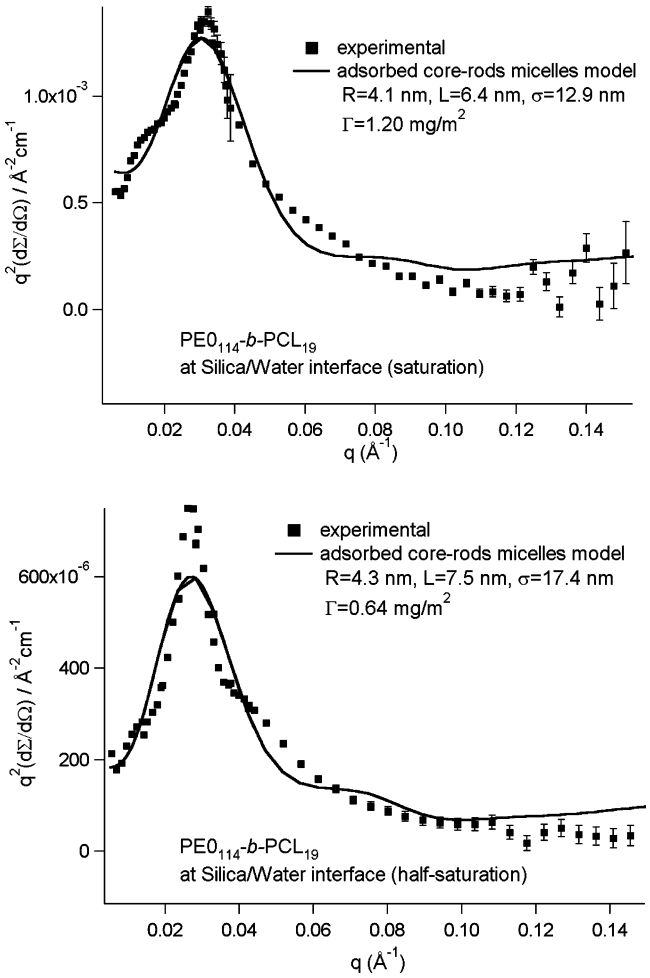

Figure 10. Fit of the SANS macroscopic cross sections to the micellar model (eqs 4−6) for the PEO_{114}-*b*-PCL_{19} copolymer and the micellar form factor for the core−rigid rods model (eq 7): (top) surface saturation; (bottom) half-saturation conditions.

Figure 10 shows that this micellar model fits the experimental data better than the models based on the direct adsorption of copolymer chains. The peak observed in the low q range (0.03 Å^{-1}) is actually accounted for, even though some discrepancy persists at very low q.

The two approaches (Guinier law and full q range) lead to consistent results for the adsorption of the copolymers on hydrophilic silica as shown in Table 4. At surface saturation, the radius of gyration is reasonable, i.e., in the 6.5−7.5 nm range, except for the PEO_{114}-*b*-PCL_8 copolymer which shows a significantly lower value (5.0 nm). The core−rods model leads to core and corona sizes similar to those obtained in solution. For instance, R = 4.5 nm and L = 6.8 nm for PEO_{114}-*b*-PCL_{19} in solution[28] compared to R = 4.1 nm and L = 6.4 nm after adsorption. The corona appears to be somewhat less extended in

(54) Higgins, J. S.; Benoît, H. C. *Polymers and Neutron Scattering*; Oxford University Press: Oxford, 1996.

Table 4. Fit of the Micelle Adsorption Model to the Experimental SANS Macroscopic Cross Sections[a]

		Guinier regime			core−rods model			
	copolymer	R_g (nm)	σ (nm)	Γ (mg/m^2)	R (nm)	L (nm)	σ (nm)	Γ (mg/m^2)
saturation	PEO_{114}-*b*-PCL_8	5.0	9.5	0.92	2.3	4.4	8.0	1.02
	PEO_{114}-*b*-PCL_{16}	6.7	12.7	1.28	3.9	7.3	12.5	1.31
	PEO_{114}-*b*-PCL_{19}	6.4	13.7	1.14	4.1	6.4	12.9	1.20
	PEO_{114}-*b*-$PMCL_{12}$	7.5	14.2	1.29	4.0	9.6	16.0	1.24
half-saturation	PEO_{114}-*b*-PCL_8	5.5	10.3	0.54	2.4	6.0	9.0	0.56
	PEO_{114}-*b*-PCL_{16}	7.1	20.1	0.62	4.0	7.9	17.5	0.63
	PEO_{114}-*b*-PCL_{19}	7.0	19.8	0.60	4.3	7.5	17.4	0.64
	PEO_{114}-*b*-$PMCL_{12}$	7.4	20.8	0.58	4.0	8.2	18.6	0.62

[a] Either the Guinier law (low q range) or the core−rigid rods model (full q range) have been used to describe the micellar form factor.

adsorbed micelles at saturation compared to solution. Moreover, the relative size of the micelles with respect to their center-to-center separation, σ, indicates that the micelles are adsorbed in a rather close-packed layer, with partial entanglement of the corona chains of adjacent micelles. However, the PEO chains remain hydrated in the surface layer as the degree of water in the corona is close to that in aqueous solution ($\phi \cong 0.15$ at the interface and in solution[28]). SANS analysis based on the micellar model leads to slightly lower amounts of adsorbed copolymer compared to the total depletion method, which might indicate the concomitant adsorption of free copolymer chains.

The radius of gyration, the core radius, and the corona thickness tend to be slightly larger at half saturation than at saturation (Table 4). For all the copolymers, the adsorbed amount is found to be close to half the value at saturation, which is consistent with the depletion method. Finally, the available area per micelle, which scales to σ^2, is approximately twice as large as that seen under saturation conditions. The larger micellar sizes are consistent with less steric constraints at lower surface coverage.

AFM Data. The morphology of the PEO_{114}-*b*-PCL_{19} copolymer adsorbed on hydrophilic silica was investigated by atomic force microscopy at two different concentrations. For this purpose, the adsorbed copolymer layer was dried (as was the case for the contact angle measurements), which may modify the structure of the micellar-like aggregates. Nevertheless, the AFM images are consistent with the persistence of micellar-like structures after drying.

At high concentration (0.6 wt %, thus in the adsorption plateau) a very rough surface is observed (Figure 11a). The very large variations in height (24−30 nm) are typical of adsorbed layers exceeding a monolayer and consisting of randomly adsorbed aggregates, with free chains possibly adsorbed between them.

At low concentration (initial copolymer solution of 0.015 wt %), the silicon wafer is no longer saturated. Figure 11b shows coexistence of spherical and poorly defined (more flat) objects, which suggests that copolymer micelles coexist with free chains. The size of these micelles, measured on height and phase images, is in the 15−20 nm range, thus of the same order of magnitude as determined by SANS.

Overall Interpretation. The experimental data reported in this paper provide information on the way PEO-*b*-P(M)CL copolymers are adsorbed at the hydrophilic silica/water interface. First of all, substitution of the ϵ-caprolactone units by a methyl group in γ position of the carbonyl has no significant effect on the adsorption process. When a hydrophobic P(M)CL block is attached to PEO, the adsorption isotherm of the copolymer on silica changes from a monolayer adsorption to a cooperative adsorption, at least above a critical copolymer concentration in water.

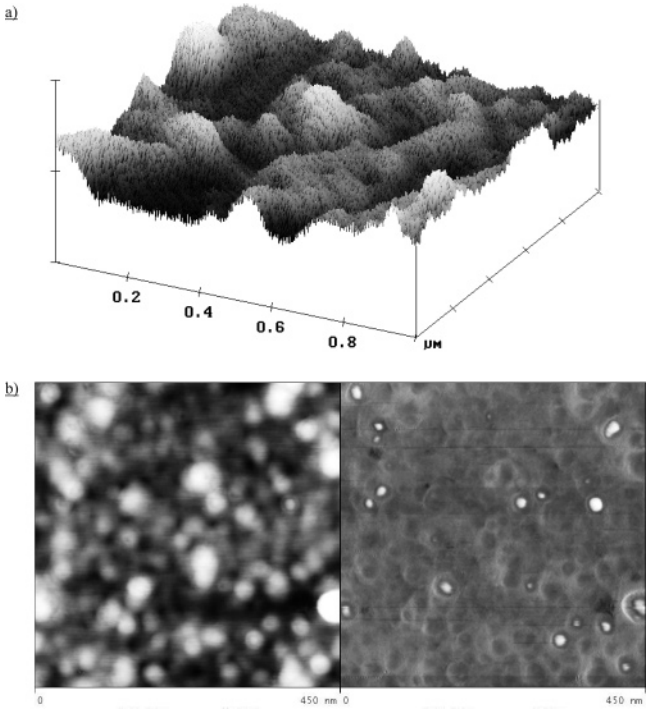

Figure 11. AFM images for the PEO_{114}-*b*-PCL_{19} copolymer adsorbed on hydrophilic silica after 1 h from (a) 0.6 wt % and (b) 0.015 wt % aqueous solution.

In this concentration regime, SANS data are reasonably well fitted by a model of adsorption of micellar aggregates, which is confirmed by AFM observations.

Dissolved in water, the PEO-*b*-P(M)CL copolymers form micelles[28] with an average diameter of ∼22 nm which are in equilibrium (slow exchange) with unimers. From SANS analysis and AFM observations, the size (diameter) for the adsorbed micelles is estimated at 12−20 nm.

The smaller micellar size at the interface compared to solution is consistent with the packing of the micelles onto silica, which also explains that the average micellar size at half saturation is slightly larger than that observed at complete coverage. The packing effects are confirmed by the PEO corona which is less extended on the surface than in bulk solution. The values of σ that govern the available surface area for the micelles, AFM topographical images of copolymer adsorbed from concentrated solutions (Figure 11a), and surface-force profiles all indicate a high copolymer density at saturation.

Several observations support the direct adsorption of the micelles formed in water: (i) the slow kinetics of adsorption, (ii) the comparable size of the micelles in solution and adsorbed on silica, and (iii) the cooperative adsorption which occurs at high concentrations (clearly beyond the cmc as determined from surface tension measurements). The PCL hydrophobicity and weak in-

teraction with silica can account for micellization before adsorption, which is driven by the well-established PEO−silica interactions (see calorimetric data). It however appears, in particular at low surface coverage, that free copolymer chains also participate in the adsorption process. Adsorption isotherms show a significant amount of adsorbed copolymer before the onset of cooperative adsorption. Contact angle and surface force measurements show that PCL is initially exposed to water and then rearranges as a consequence of free copolymer chains eager to adopt a conformation of lower free energy.

Despite lack of interaction between P(M)CL and hydrophilic silica, the adsorbed amount of copolymer increases with the hydrophobic molecular weight. In aqueous solution, the aggregation number increases with the hydrophobic block length, whereas the size of the micelles remains nearly constant.[28] Therefore the micellar volume fraction increases with the size of the hydrophobic block, which explains why the adsorbed amount is larger for longer P(M)CL blocks.

Conclusions

This study dealt with the adsorption of PEO-*b*-P(M)CL block copolymers consisting of a hydrophilic PEO block and various (shorter) hydrophobic P(M)CL blocks on glass and silica. Compared to homoPEO, the P(M)CL block enhances the adsorption as confirmed by a transition from a monolayer adsorption for PEO to a cooperative adsorption of micellar aggregates and by a substantial increase of the adsorbed mass above the cmc.

In aqueous solution, the copolymers form, above the cmc, micelles that are in equilibrium with slowly exchanging free chains (unimers). Below the concentration at which the cooperative adsorption occurs (C_c), there is a preference for the adsorption of unimers, which expose PCL, at least partly, to contact with water. Above C_c, the micelles are then adsorbed without significant modification of their size, except for a small contraction due to their packing on the surface. The unimers have to organize in the presence of these bulkier objects, resulting in the removal of some PCL/water contacts after a slow reorganization process. This picture is qualitatively supported not only by the techniques that probe the adsorbed layer in aqueous medium (FMC, SANS, MASIF) but also by techniques that analyze the copolymer layer after separation of the silica substrate from water and subsequent drying. Therefore, the system that reorganizes slowly in water is not able to do the same in air during the short drying time. The main reasons are likely the low mobility of the polymer chains and the small driving force for P(M)CL blocks to migrate and expose themselves to air at the expense of PEO.

Acknowledgment. The authors are grateful to Dr. G. Broze for access to the FMC equipment at Colgate-Palmolive R&D (Liège, Belgium). They are very much indebted to the "Fonds pour la Formation à la Recherche dans l'Industrie et l'Agriculture" (F.R.I.A.) for a fellowship to P.V., to the "Politique Scientifique Fédérale" for general support to CERM in the frame of the "PAI V/03: Supramolecular Chemistry and Supramolecular Catalysis", and to the European Commission Access to Research Infrastructures Action of the Improving Human Potential Program (HPRI) for financial support and access to the Forschungszentrum (Jülich) ("Jülich Neutrons for Europe") and the Laboratoire Léon Brillouin (Saclay, France) (Contract HPRI-CT-1999-00032).

Supporting Information Available: Derivation of the macroscopic scattering cross section for spherically symmetric micelles adsorbed onto a randomly oriented solid surface and a figure showing the vectors used to define the locations of the scatterers in eq A2. This material is available free of charge via the Internet at http://pubs.acs.org.

LA047425+